Graded Nanostructures Produced by Sliding and Exhibiting Universal Behavior

D. A. Hughes [1,*] and N. Hansen [2]

[1] *Sandia National Laboratories, MS 9405, P.O. Box 969, Livermore, California 94551-0969*
[2] *Materials Department, Risø Laboratory, P.O. Box 49, DK4000 Roskilde, Denmark*

(Received 7 March 2001; published 10 September 2001)

Nanostructured copper was produced by deformation under large sliding loads. In the near surface layers, 10 nm scale microstructures form and coarsen with increasing depth from the surface. The graded structure enables characterization of the structural scale over several orders of magnitude. Analysis reveals that universal scaling of the microstructure exists from 10 000 to 10 nm. The limit of scale is pushed to an order of magnitude of the ultimate scale at which the crystallinity is lost. This universality opens the door for easy manufacture of ever finer scale components by deformation.

DOI: 10.1103/PhysRevLett.87.135503 PACS numbers: 61.72.Ff, 62.20.Fe, 62.25.+g, 81.05.Bx

The demand for very fine scale components is dramatically increasing for a number of technologies that utilize micromechanical devices. To optimize properties, including ductility and strength, it has been proposed that many of those devices be constructed from metals and alloys whose microstructure scales from submicrometers to nanometers. Such metals are very difficult to produce, but cold deformation is a promising route. Large plastic deformation (strain) is required since even a 100 times thickness reduction in plate rolling of Al, Cu, or Ni can only bring the scale of the microstructure down to about 100–200 nm. A way to obtain extreme degrees of deformation is to press metal parts together and slide them against each other. During the sliding, the surface asperities or ridges of the harder metal act as a miniature plow or bulldozer to push up and then flatten a wave of the softer metal [1,2]. As this wave is flattened its surface is shifted forward from the underlying layers producing a shear strain estimated near 3. As the parts continue to slide the quick passage of successive ridges intensifies this deformation. Although this process was conceived within the context of friction and wear [3], we use it here as a quick and easy tool to create very fine graded microstructures.

Formation and retention of these structures depends on sample and counterface materials as well as on asperity shape and pattern. We describe results from malleable high purity Cu (99.99%) block samples with an initial annealed grain size of 100 μm and flat hardened steel counterfaces. The final Cu structure is stabilized by the solution of 1% Fe (and possibly O from air) into the near surface regions, 0 to 6 μm deep, diffusing from the counterface in the deformation process. This *in situ* alloying inhibits recrystallization of the fine structure which can occur in highly deformed pure Cu at room temperature [4].

A unique single-pass flat-plate friction tester was used as described in Ref. [5]. The steel counterface was blanchard ground to produce roughly parallel sets of ridgelike asperities with a 130 μm wavelength and 5°–10° inclination angle. During deformation ~1000 asperities plow the surface of the Cu. The combination of hard shallow steel asperities and malleable Cu enables this process to produce very large strains below the surface, while minimizing fracture and galling of the Cu. Note that the sample blocks have a thickness of 1 cm that is much deeper than the surface deformation zone of ~300 μm. The large normal pressures and short sliding distance of 127 mm distinguish this process from typical friction and wear tests.

A view of the nanostructures produced in the surface layers of the Cu friction samples is obtained at high magnification by transmission electron microscopy (TEM) (Fig. 1). Friction surfaces are marked and protected by Ni electroplating after deformation and prior to cross sectioning. The cross sections show finely spaced and roughly planar boundaries parallel to the surface. Just below the surface, as illustrated by the tracing of the structure (Fig. 1), a distribution of boundary spacings is observed, from 3–30 nm with an average of 12 nm (spacings, D^{GNB}, are measured perpendicular to the boundaries). We have previously classified these extended boundaries as geometrically necessary boundaries (GNB).

These boundaries separate crystal volumes that are rotated with respect to one another. The extended boundaries provide a spatially intermixed distribution of low ($<4°$) to high ($>15°$) angle boundaries. The defect structure between the boundaries is clearly resolved for spacings above 30 nm. While much of this volume is nearly dislocation free, short dislocation boundaries and a few isolated dislocations are observed bridging the flat extended boundaries (Fig. 1). The short bridging dislocation boundaries are low angle boundaries. A few deformation-induced twins are observed (Fig. 1) as well as unresolved features bridging the narrowest boundary spacings. These latter features may be stacking faults.

As one views the layers farther below the surface, scanning from left to right in Fig. 1, the same morphology is observed albeit with a larger spacing between the extended boundaries. This graded structural size is illustrated both microstructurally and quantitatively in Figs. 1 and 2. The average spacing, $D_{\mathrm{av}}^{\mathrm{GNB}}$, increases from 50 to 170 nm with depths from 2 to 20 μm. Extended

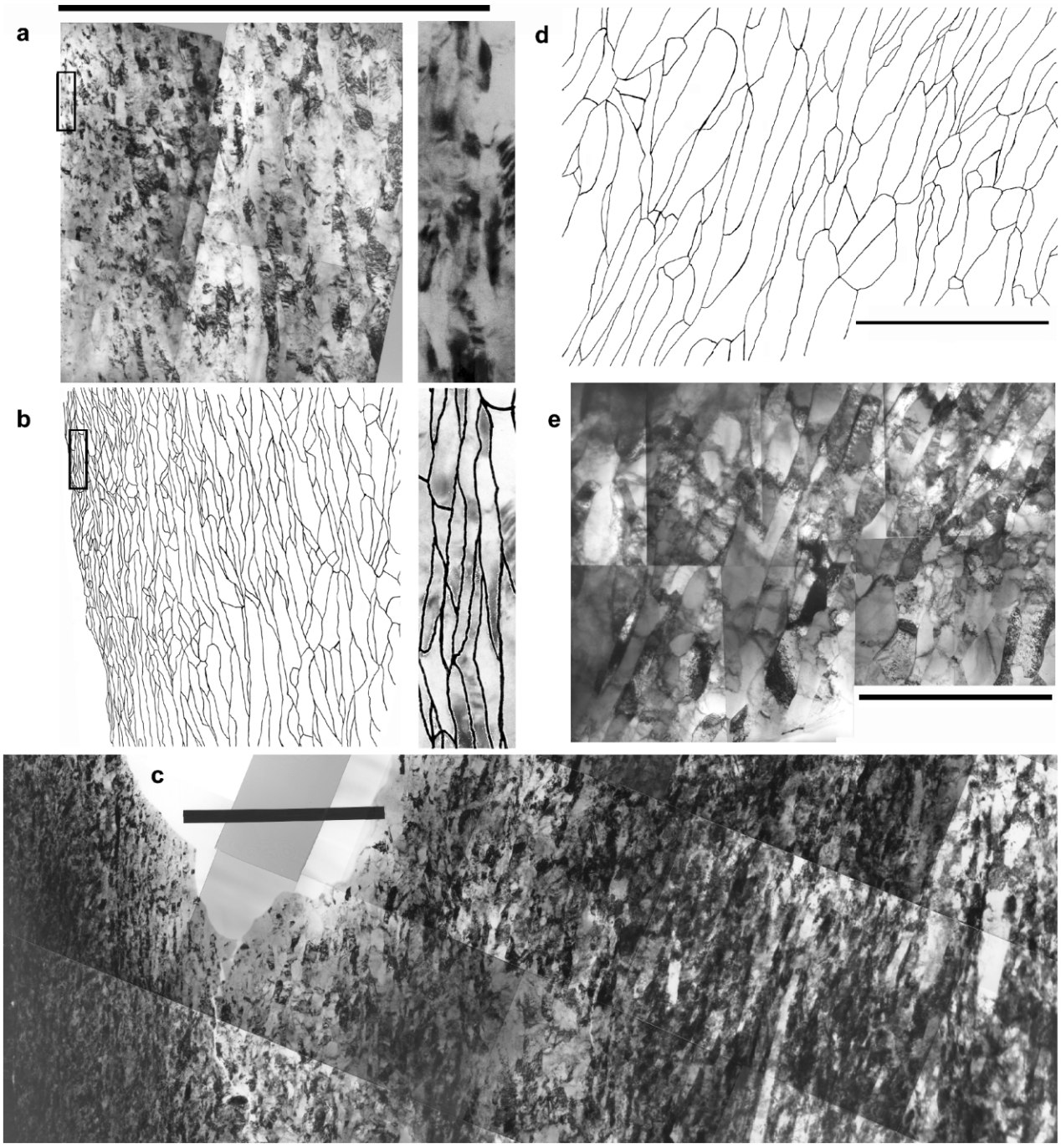

FIG. 1. Graded nanostructures produced by friction deformation as viewed in cross section by TEM. (a) Micrograph and (b) tracing of extended boundaries in Cu following sliding under 12 MPa applied normal pressure; the left side is coincident with the surface. Rectangular boxes show location of the adjacent high magnification excerpts illustrating a layer with 12 nm average boundary spacing. These rectangles are 70 nm wide. (c) Following sliding with 22 MPa pressure; the surface is coincident with the left side. (The pale gray region underneath the scale marker is the hole produced when making the TEM foil.) (d) Tracing and micrograph (e) of sample in (a) but at 20 μm below the surface. Scale markers are 2 μm.

boundaries consist of a spatial intermixture of low to high angle boundaries (see also Ref. [6]) with the average angle of all boundaries decreasing with increasing depth. Short low angle dislocation boundaries bridge between them.

At much larger depths, 100–200 μm, below the surface, where the strain is low, long extended boundaries are also observed but they are inclined to the surface and have a relatively large spacing of 1–2 μm. The extended boundaries have low to medium angles. High angle boundaries are no longer observed except as the original grain boundaries. Between these extended boundaries, approximately equiaxed cells are found and defined by short dislocation boundaries. The cell interiors are fairly free of

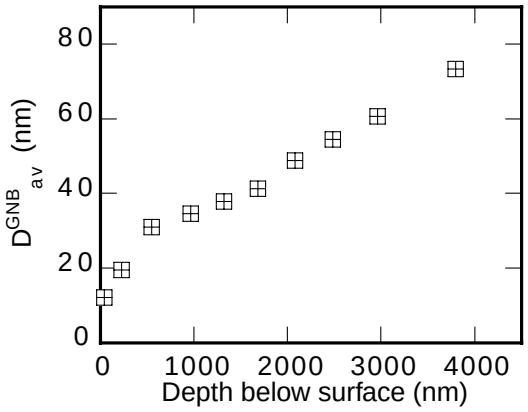

FIG. 2. Average boundary spacing $D_{\mathrm{av}}^{\mathrm{GNB}}$ vs depth for a friction sample with 12 MPa normal pressure.

dislocations. Cell boundaries consist of low angle boundaries and their dislocation character is clear.

Close estimates of the strains in the different layers can be made based on the accurate microstructural measurements and the continuous reduction in spacing. The reduction is analyzed quantitatively by introducing the increase in boundary area per unit volume, S_v, as a structural parameter. For layered planar structures $S_v = 1/D_{\mathrm{av}}^{\mathrm{GNB}}$ [7]. In experiments in which strains can be measured well, i.e., rolling and torsion, a power law relationship is observed, in fcc metals, between S_v and effective von Mises strain, ϵ_{vM}, up to 5 (i.e., a reduction in thickness of $\sim$100) (Fig. 3). Different exponents in the power law are observed for different materials as shown by the two examples in Fig. 3. Note that in Fig. 3 the data for rolled Cu are from [8] and that for torsion deformed Cu are from [9]. Strain is estimated based on an extrapolation of these power laws

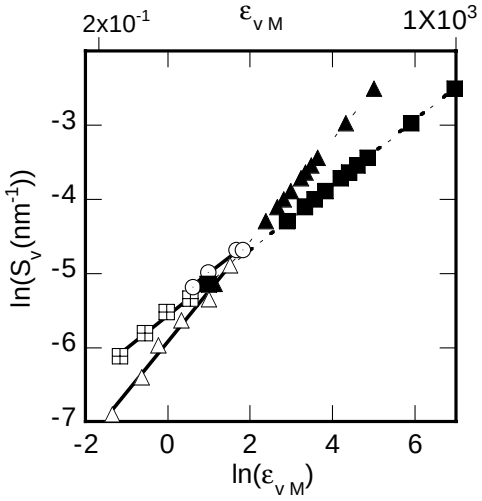

FIG. 3. Extrapolation of the power law relationship between boundary area per unit volume S_v and strain. Strain extrapolations for friction data (solid symbols) are based on other experiments in rolled Ni (open triangles), rolled Cu (open circles), and torsion deformed Cu (open squares).

using the friction spacing data. Strain from this extrapolation overlaps, at larger depths and smaller strains, the strain measurements estimated from shear offsets produced in preexisting twin boundaries perpendicular to the surface (e.g., see Ref. [5]). Strain levels at the surface are $>$100.

The continuous internal morphological progression in the high to low strain layers of the friction sample is next compared to deformation structures obtained by rolling. Even extensive deformation by rolling is limited to strains near 5. Thus direct comparisons between friction and rolling is limited to the deeper layers in friction. Rolling structures have been extensively studied in medium to high stacking fault energy metals: Al, Cu, and Ni. A similar morphological evolution has been observed for these metals. Minor solid solution additions to these pure metals only refine the structure without significant morphology changes. Since the most comprehensive large strain studies were performed on Ni [10], they are used for comparison. We believe a comparison with bulk deformation behavior is valid due to the fineness of the structure observed in the near surface layers. Previous experiments have shown that a ratio of grain size versus specimen size of 1 to 10–15, eliminates surface effects on the mechanical properties of the whole specimen [11].

In both friction and rolling, as described above, two types of boundaries are observed: the flat extended boundaries and the bridging short low angle dislocation boundaries. The inclination of the extended boundaries with respect to the sample deformation in both rolling and friction shows a transition from a high inclination at low strain to one that is parallel at high strain. Of particular interest with respect to the similarity are the flat extended boundaries having a unique spatial intermixture of low to high misorientation angles. This morphological similarity appears to indicate that the same underlying slip and shear mechanisms are controlling the microstructure evolution from strains of 0.1 to $>$100.

To more rigorously test this hypothesis, note that the boundary tracings showing a distribution of sizes within a given layer in friction and rolling look alike. This similarity inspires a scaling analysis of the friction structure. It has been found in a monotonic deformation that the probability distributions $p(D^{\mathrm{GNB}}, D_{\mathrm{av}}^{\mathrm{GNB}})$ of individual perpendicular spacings, D^{GNB}, between the extended boundaries, at a given strain level or condition, can be scaled by their average spacing, $D_{\mathrm{av}}^{\mathrm{GNB}}$, into a single universal distribution [12]. Thus, $p(D^{\mathrm{GNB}}, D_{\mathrm{av}}^{\mathrm{GNB}}) = (D_{\mathrm{av}}^{\mathrm{GNB}})^{-1} f(D^{\mathrm{GNB}}/D_{\mathrm{av}}^{\mathrm{GNB}})$ is a simple function of the average spacing.

Accordingly spacings were measured in narrow layers parallel to the surface as a function of depth. The probability distributions of these spacings within a given layer (i.e., average strain level) normalized by their individual average spacings are plotted in Fig. 4. Following this normalization, all of the distributions collapse into the same universal distribution as before, thereby extending its range of applicability 1 order of magnitude in average spacing

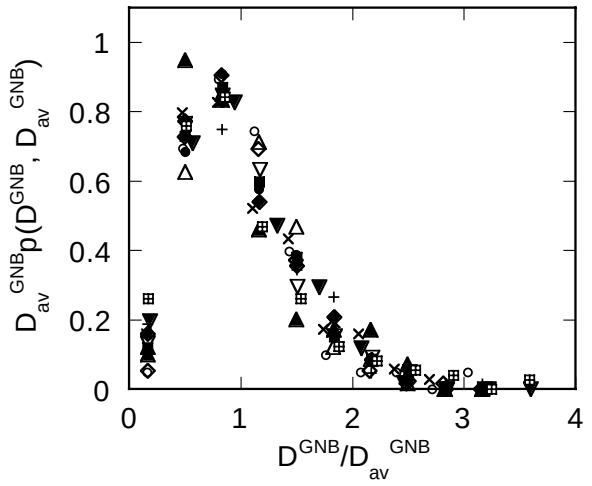

FIG. 4. Probability distributions of nanometer scale boundary spacings produced by friction as a function of depth normalized by their average spacing (see Fig. 2) compared to distributions at larger scales in rolled Ni. Friction, open circles: $D_{av}^{GNB} = 12$ nm; open squares: $D_{av}^{GNB} = 19$ nm; open diamonds: $D_{av}^{GNB} = 31$ nm; open up triangles: $D_{av}^{GNB} = 35$ nm; open down triangles: $D_{av}^{GNB} = 38$ nm; solid circles: $D_{av}^{GNB} = 41$ nm; solid squares: $D_{av}^{GNB} = 49$ nm; solid diamonds: $D_{av}^{GNB} = 55$ nm; solid up triangles: $D_{av}^{GNB} = 61$ nm; solid down triangles: $D_{av}^{GNB} = 73$ nm; squares with cross: $D_{av}^{GNB} = 171$ nm; plus sign: Ni 70% reduction, $D_{av}^{GNB} = 280$ nm; and cross: Ni 98% reduction, $D_{av}^{GNB} = 133$ nm.

and in strain level. Strikingly, the scaling of the spacing distributions holds over nearly 3 orders of magnitude in spacing and strain level.

This universal scaling, coupled with the continuous reduction in average spacing with increasing deformation, indicates that there is a continuity of the processes which create new boundaries and those that remove them, from low to very high strain. These processes are dislocation slip, short range dislocation interactions, and longer range interactions between the boundaries. Since deformation and microstructural evolution occurs by dislocation slip processes in rolled metals, the universal scaling of the friction nanostructures indicates the continuation of the underlying slip processes even to 10 nm structures at extreme strains. We thereby explore a scale not accessible to conventional deformation experiments, in which the lower limit is about 100 nm, or atomistic calculations, in which the upper limit is about 10 nm [13]. Our results push the limits of scale and boundary spacing within an order of magnitude of the ultimate size limit at which we expect crystallinity to be destroyed.

The reduction in size with estimated strain shows a continuous refinement without saturation, demonstrating clearly that cold deformation processes have the potential to produce microstructures with characteristic spacing down to 10 nm following very high strains. An order of magnitude decrease in size is realized by adapting this friction process compared to other bulk deformation processes (e.g., rolling, equal channel angular pressing, drawing, and accumulative roll bonding [14]). The continuous structural refinement and evolution observed creates possibilities for tailoring a fine structure in the range from μms to nms by proper selection of the deformation process condition. The proven extrapolation of the microstructure to the nanoscale is assumed to be paralleled by a significant increase in strength. We have not been able to underpin this suggestion by experiment as the spatial resolution of current techniques (e.g., nanoindentation) is much larger than the scale of the microstructure layers. Rather this assumption is based on the behavior of nanostructured materials produced by other methods. For example, in Cu samples produced by gas condensation and warm compaction, the hardness values show a continuous increase with a decrease in boundary spacing down to 15 nm [15]. Deformation under a large sliding load therefore has potential as a versatile process for the manufacture of fine scale components of complex shape for application in the microelectronic, medical diagnostic, and implant industries.

D. A. H. acknowledges the support of the U.S. DOE Office of Basic Energy Sciences, Division of Materials Sciences under Contract No. DE-AC04-94AL85000.

*Electronic address: darcyhu@sandia.gov

[1] N. Bay, T. Wanheim, and A. S. Petersen, Wear **34**, 77 (1975).
[2] J. M. Challen and P. L. Oxley, Wear **53**, 229 (1979).
[3] D. A. Rigney and J. P. Hirth, Wear **53**, 345 (1979).
[4] J. Gil-Sevillano, P. van Houtte, and E. Aernoudt, Prog. Mater. Sci. **25**, 69 (1980).
[5] D. A. Hughes, D. B. Dawson, J. S. Korellis, and L. I. Weingarten, Wear **181**, 458 (1995).
[6] P. Heilmann, W. A. T. Clark, and D. A. Rigney, Acta Metall. **31**, 1293 (1983).
[7] E. E. Underwood, *Quantitative Stereology* (Addison-Wesley Publishing Co., Reading, MA, 1970).
[8] H. Hu, in *Textures*, edited by J. Grewen and G. Wassermann, Research and Practice Vol. 200 (Springer-Verlag, Berlin, 1969).
[9] J. Alberdi, Universidad de Navarra Facultad de Ciencias, San Sebastian, Grandes Deformaciones Plasticas en Frio en Policristales de Cobrey Aluminio (Torsion), 1984.
[10] D. A. Hughes and N. Hansen, Acta Mater. **48**, 2985 (2000).
[11] N. Hansen, Acta Metall. **25**, 863 (1977).
[12] A. Godfrey and D. A. Hughes, Acta Mater. **48**, 1897 (2000).
[13] J. Schiotz, F. D. Di-Tolla, and K. W. Jacobsen, Nature (London) **391**, 561 (1998).
[14] *Ultrafine Grained Materials*, edited by R. S. Mishra, S. L. Semiatin, C. Suryanarayana, N. N. Thadani, and T. C. Lowe (The Minerals, Metals and Materials Society, Warrendale, 2000).
[15] P. G. Sanders, J. A. Eastman, and J. R. Weertman, Acta Mater. **45**, 4019 (1997).